

# Surface effects on Young's modulus and hardness of fused silica by nanoindentation study

Lianqing Zheng · Ansgar W. Schmid ·  
John C. Lambropoulos

Received: 14 November 2005 / Accepted: 4 January 2006 / Published online: 23 November 2006  
© Springer Science+Business Media, LLC 2006

**Abstract** The surface Young's modulus ( $E$ ) and hardness ( $H$ ) of fused silica samples have been studied by nanoindentation. Two factors strongly affect the results of  $E$  and  $H$ . One factor is the polishing quality of the fused silica surface. Poor polishing quality produces much smaller  $E$  and  $H$  than the literature values for bulk fused silica. The second factor is surface flatness. Even for a well-polished silica surface, an "arch bridge effect" may hinder the measurements of the true values of  $E$  and  $H$ . A correction procedure is proposed to eliminate this effect, and the corrected results show substantial improvements.

## Introduction

Conventional pitch polishing of a standard glass, such as fused silica, is not expected to affect the glass's mechanical properties. Indeed, polishing is designed and expected to remove any subsurface damage from

the glass surface and/or any residual stresses, thus returning the material surface to a pristine condition. Such damage and residual stresses are remnants of earlier grinding cycles in which they were generated. A polishing cycle is thus designed so that sufficient damaged or stressed material is removed from the surface. The classic textbooks by Izumitani [1] and Karow [2] describe the generation of subsurface damage and residual stresses during the grinding cycle of glass surfaces. Correlations between the damaged or residually stressed surface layers and the glass near-surface mechanical properties have been described by Lambropoulos et al. for many optical glasses [3–6].

Near-surface mechanical properties of glasses have traditionally been measured using microindentation methods, such as Knoop or Vickers microindentation [7]. On the other hand, it is usually assumed that the near-surface elastic properties—for example, Young's modulus or shear modulus—are the same as the material's bulk elastic properties. One reason for such an assumption is that near-surface elastic properties are more difficult to measure, especially when the near-surface layers are in the range of a few  $\mu\text{m}$  or less. With the advent of nanoindentation, however, both elastic modulus and hardness can now be measured with sufficient accuracy in depths ranging from  $\mu\text{m}$  to nm from the material surface [8]. Thus, nanoindentation allows the direct measurement of near-surface mechanical properties and can address the question of what effect polishing process conditions have on these properties. Equivalently, nanoindentation may be seen as a means of monitoring the mechanical state of the polished surface.

We describe in this report a series of measurements of Young's modulus and hardness by nanoindentation

---

L. Zheng · J. C. Lambropoulos (✉)  
Department of Mechanical Engineering and Laboratory for  
Laser Energetics, University of Rochester, 250 E. River  
Road, Rochester, NY 14623-1299, USA  
e-mail: jcl@me.rochester.edu

A. W. Schmid  
Laboratory for Laser Energetics, University of Rochester,  
250 E. River Road, Rochester, NY 14623-1299, USA

*Present Address:*  
L. Zheng  
Department of Chemistry, University of Missouri-Columbia,  
Columbia, MO 65211, USA

on fused silica samples of high aspect ratio in which one side was conventionally pitch polished. We first demonstrate that conventional microindentation hardness (e.g., Knoop) is not affected by the polishing process. We then show that, depending on the polishing process conditions, it is possible to generate two sources of error on the nanoindentation-measured mechanical properties. The first source of error is due to the state of the polished surface as measured, for example, by the duration of the polishing cycle or the amount of material removed. The other source of error is the “arch bridge effect” whereby samples with high aspect ratio, following polishing, can exhibit a significant amount of bowing. The effect is that nanoindentation senses a composite stiffness consisting of the inherent elasticity of the glass surface (measured by the Young’s modulus) and of the elastic stiffness of a simply supported beam bending due to the applied nanoindentation load. We demonstrate how such errors may be addressed.

## Experimental procedures

### Sample preparation

Four fused silica specimens were tested. All specimens, with fine-ground surfaces, were manufactured by Glass Fab, Inc. (Rochester, NY) to Corning 7980 quality with a size of  $77 \times 25 \times 6$  mm. All samples were conventionally continuously pitch polished on the same pitch at an optical fabrication shop [Center for Optics Manufacturing (COM), University of Rochester]. Hastilite PO was used as the polishing compound. Only one  $77 \times 25$  mm side of each sample was polished and subsequently used to measure  $E$  and  $H$ . Before each polishing, that surface was reground to remove all prior indents made by the nanoindenter. All samples were polished three times for different durations: 17 h, 22 h, and 1 week, respectively. No polishing work had been done on the samples prior to the first polishing. After each polishing, the polished surfaces of fused silica specimens were cleaned using methanol, then tested in the nanoindenter for  $E$  and  $H$ . Special marks were used on the side surface of each sample to ensure that the appropriate surface was polished and tested.

### Nanoindentation test

All nanoindentation tests were performed using a Nano Indenter® IIs system at COM. The indenter is a Berkovich type. For a complete and detailed description of the structure and specifications of this nanoind-

enter and procedures of the indentation test, see Ref. [9]. The system’s load and displacement resolutions are  $\pm 0.1 \mu\text{N}$  and  $\pm 0.04$  nm, respectively. Proper calibrations of this instrument were performed immediately prior to any indentation test. The indentation test procedure consists of six steps: Approach Segment, Load Segment, Hold Segment, Unload Segment, Hold Segment, and Unload Segment. In the Approach Segment (A), the indenter moves down to determine the “zero” position for load and displacement. Then load is applied in the Load Segment (LL) at a constant rate of  $35,000 \mu\text{N/s}$  until it reaches its maximum  $350,000 \mu\text{N}$ . The indent is held in the Hold Segment (H) at  $350,000 \mu\text{N}$  for 10 s, followed by the Unload Segment (UL) in which the load is removed with a rate of  $-35,000 \mu\text{N/s}$  until it reaches  $35,000 \mu\text{N}$ . Another Hold Segment is then applied at this load, and 2 points (i.e., a load–displacement pair) are logged every second until a total of 50 points have been accumulated. Finally, in the second Unload Segment, the residual load is completely removed with a rate of  $35,000 \mu\text{N/s}$ .

A schematic of the distribution of the indents on a fused silica sample is shown in Fig. 1. To avoid interfering with future work performed in the middle of the sample (e.g., laser irradiation), all indents were close to, but far enough away from, edges to avoid possible edge effects. As shown in Fig. 1, the indents were divided into six groups along the  $X$  axis with 11 indents in each group along the  $Y$  axis. Spacing was 4 mm along the  $Y$  direction and 1 mm along the  $X$  direction, but the distance between group 3 and group 4 was 12 mm.

### Knoop microindentation test

Knoop microhardness of samples 1 and 2 was measured in a Tukon® Microhardness Tester (Instron Corporation). On sample 2, loads of 10, 25, 50, 100, and 200 g were used, while only 50 g was applied on sample 1. Thirty-three indentations were made approximately along the lines of group 2 and group 5 on sample 1, and 15 on sample 2 under each load with randomly chosen positions. The loading duration was 30 s.

## Results

Earlier, Young’s modulus and Berkovich hardness of Corning 7940 UV-grade A fused silica were reported to be 71.5 and 9.22 GPa, respectively [9], which were obtained with the same nanoindentation procedure. In the product literature for HPFS® Corning code 7980, Young’s modulus is reported to be 72.7 GPa [10].

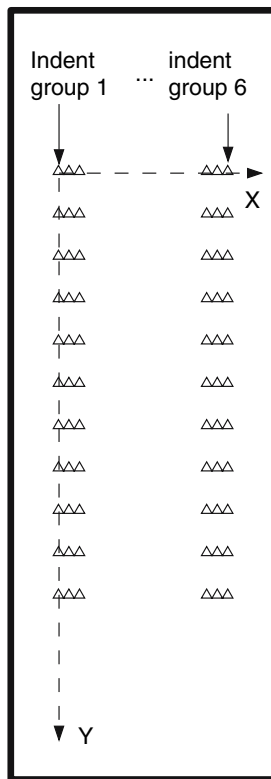


**Fig. 1** Schematic of indent distribution on a fused silica specimen. Triangles represent indents. Sixty-six indents are divided into six groups with 11 in each group. Group 1 is 4.5 mm away from the left edge of the specimen, and indents at  $Y = 0$  are 18.5 mm away from the upper edge. Spacing between two adjacent groups is 1 mm, but group 3 and group 4 are separated by 12 mm. Spacing in the  $Y$  direction is 4 mm

Figures 2 and 3 show the distributions of Young's modulus and Berkovich hardness of four fused silica specimens after the first polishing of 17 h, respectively. Young's modulus on all of the samples varied with position from  $\sim 10$  GPa to  $\sim 60$  GPa. Variations were seen along both the  $X$  and  $Y$  directions, but with different patterns on different samples. On sample 1,  $E$  increased along the  $Y$  axis but decreased along the  $X$  axis. With increasing  $Y$  coordinate, the differences along the  $X$  axis became larger (from approximately 2 to 26 GPa). Sample 4 was similar to sample 1 with a smaller change in  $X$  direction. Sample 3 would also have had a similar pattern if we had put the sample in reverse such that  $Y = 0$  mm became  $Y = 40$  mm and indent group 1 became group 6. Sample 2 looked different from the other samples. Though  $E$  also decreased along the  $X$  direction, its variation along the  $Y$  direction was much smaller.

The Berkovich hardness of fused silica had similar distributions as Young's modulus on each sample.

Generally the larger the Young's modulus, the larger the hardness. The values of hardness changed from 1.3 to 8.8 GPa with position. Due to the similar patterns of  $E$  and  $H$ , only the spatial distribution of  $E$  is reported for the second and third polishings.

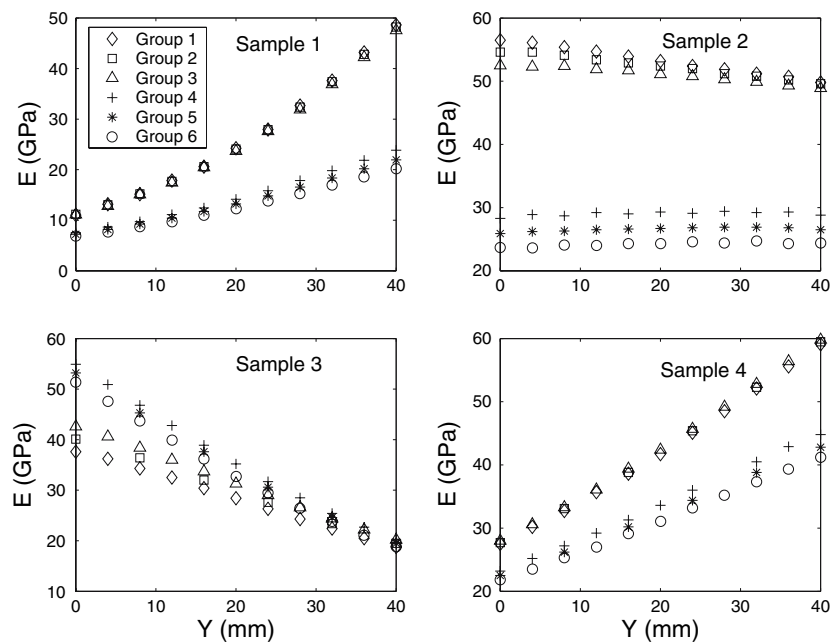
To find the reason for these large variations of  $E$  and  $H$  and discrepancies of their values from those in the literature, a standard fused silica sample of  $12.7 \times 12.7 \times 6.4$  mm, which came with Nano Indenter® IIs, was tested with the same nanoindentation procedure as described in Section "Experimental procedures". From 30 indents, we obtained a Young's modulus of  $68.8 \pm 0.2$  GPa and a Berkovich hardness of  $9.54 \pm 0.04$  GPa. This result ruled out the possibility that there was any system problem in the nanoindenter itself.

Table 1 shows the results of Knoop microhardness of fused silica from our experiment and Ref. [7]. Considering the different grades of fused silica tested, different instruments and testing conditions, our results are in good agreement with those of Hirao and Tomozawa. Shown in Fig. 4, Knoop microhardness of sample 1 is randomly distributed around the mean value. The pattern of hardness variation found for nanoindentation in sample 1 is not found for Knoop microhardness. This result underscores that the traditional microhardness test may not reveal some characteristics of the solid surface that only the nanoindenter is able to probe.

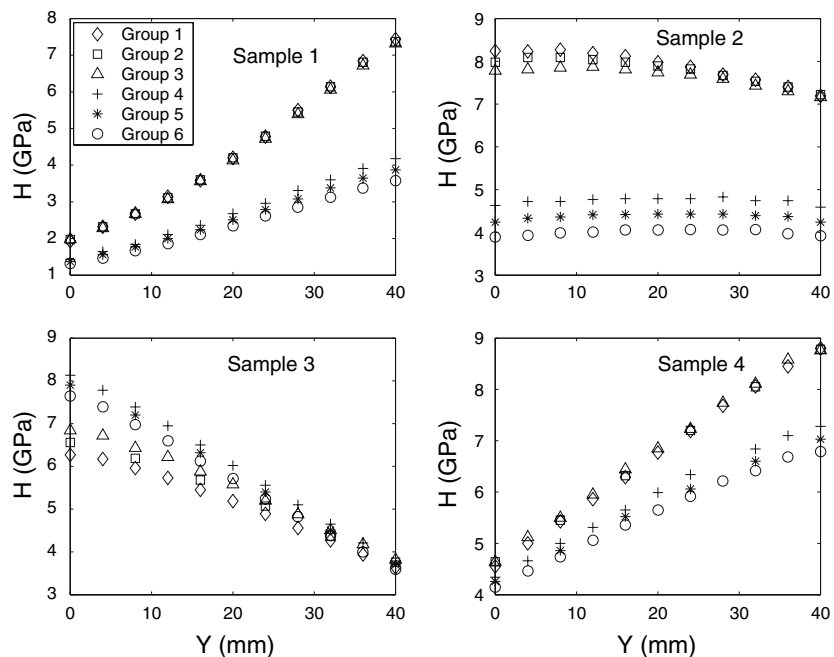
The nanoindenter load–displacement curves for typical indents on our sample and on the standard fused silica sample are compared in Fig. 5. Under the same loading conditions, indenter displacement in our sample was much larger with a maximum of more than 4,000 nm, while the maximum displacement in the standard sample was less than 1,800 nm. During the Hold Segment (H), the indenter crept under a constant load. Compared to a creep deformation of about 10 nm in the standard fused silica, the creep distance in the Hold Segment right after the Load Segment (LL) on our sample was more than 350 nm. A larger indenter displacement produced a smaller Young's modulus and hardness, i.e. the material appeared "softer." Since the nanoindenter measures the near-surface Young's modulus and hardness, the quality of the polished surface of these fused silica samples was questioned. To investigate this problem, we performed a second polishing with a 22-h duration.

The Young's modulus of all fused silica samples after the second polishing are shown in Fig. 6. Its range of variation became much smaller, from approximately 42 to 62 GPa, and its average was closer to the literature value. Berkovich hardness (not shown) had

**Fig. 2** Distributions of Young's modulus on fused silica specimens after the first polishing (17 h). On most specimens,  $E$  varied monotonically along both the  $X$  and  $Y$  directions. Each sample had its own pattern of distribution, and the values of  $E$  varied from approximately 10 to 60 GPa



**Fig. 3** Distribution of Berkovich hardness of fused silica specimens after the first polishing (17 h). Hardness had similar patterns of variation as Young's modulus, and its values changed with different positions from 1.3 to 8.8 GPa



similar changes. From this perspective, the quality of the polished surface of fused silica specimens was greatly improved; however, each sample still possessed its own pattern of variation in  $E$  and  $H$ .

Though a major improvement was achieved after the second polishing, the Young's modulus and hardness were still 20 and 10% lower than the literature values, respectively. The third polishing was performed to obtain further improvement. This continuous pol-

ishing lasted for 1 week. The results for Young's modulus are presented in Fig. 7. Further improvements, such as less variations and better average values were observed. A similar distribution of Young's modulus, which appeared on samples 2, 3, and 4, was that the variations of  $E$  along the  $Y$  axis were symmetric about  $Y = 20$  mm, at which the minima were located.  $E$  became smaller at first and then larger after the turning point at  $Y = 20$  mm. This intriguing

**Table 1** Knoop microhardness of fused silica

Load (g)	Knoop microhardness (GPa)	
	Present study	Ref. [7]
10	9.03 ± 0.93 <sup>a</sup>	>6.57 <sup>c</sup>
25	7.48 ± 1.00 <sup>a</sup>	5.88–6.47 <sup>c</sup>
50	6.48 ± 0.27 <sup>a</sup> , 6.52 ± 0.39 <sup>b</sup>	5.93 <sup>d</sup>
100	6.28 ± 0.15 <sup>a</sup>	5.49–5.88 <sup>c</sup>
200	6.10 ± 0.06 <sup>a</sup>	5.36 <sup>d</sup>

<sup>a</sup> Sample 2, loading duration = 30 s  
<sup>b</sup> Sample 1, loading duration = 30 s  
<sup>c</sup> Estimated from Fig. 3 in Ref. [7], loading duration = 900 s  
<sup>d</sup> Estimated from Fig. 2 in Ref. [7], loading duration = 30 s

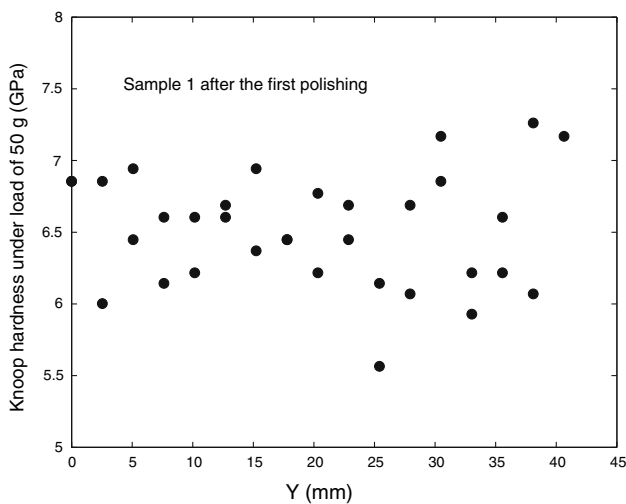


**Fig. 4** Distribution of Knoop hardness of fused silica sample 1 after the first polishing. The pattern of variation in hardness found for nanoindentation is not found for Knoop microhardness

pattern differed from those obtained from previous polishing and should be caused by different factors.

Table 2 provides the mean values and standard deviations of Young’s modulus and Berkovich hardness of all samples after each polishing, compared with those from the standard fused silica sample and the literature. After each polishing, distributions of *E* and *H* became more uniform on each specimen and between specimens. Their averages also approached the literature values and those of the standard sample. However, even after the third polishing, the Young’s modulus was still about 15% smaller than the literature and standard sample values. Further polishing work was not expected to improve this condition by much; therefore factors other than polishing were affecting these results. One such factor was discovered by inspecting the distributions of *E* after the third polish-

ing and by measuring the flatness of the samples using an interferometer.

The flatness of surfaces on which nanoindentation tests were performed was measured using a Zygo GPI XP interferometer after the third polishing. For all the specimens, the highest part was found at the center of the samples, while the shorter edges were the lowest. This flatness made the sample look like an arch bridge, and the height of the “bridge,” i.e., the peak-to-valley (*P*–*V*) difference of the flatness, ranged from 2.2 to 3.6 μm for different samples. Due to this arching structure, when the nanoindenter applies load to the sample, the sample deforms like a simple edge-supported beam subject to a transverse load. The deflection of the sample is superimposed on the displacement of the indenter, producing a larger displacement and resulting in a lower Young’s modulus and hardness [11]. For an indent near the sample center, the deflection of the sample was larger than one produced by an indent closer to the shorter edges of the sample and the measured Young’s modulus became smaller. This is in agreement with Fig. 7. In the next section, a correction method is proposed to account for the effect of sample deflection, further improving the results for Young’s modulus and Berkovich hardness.

**Analysis**

To eliminate the deflection effect of a fused silica specimen caused by its arch bridge structure, we at first study how Young’s modulus and hardness are calculated from the load–displacement (*P*–*h*) curve (see Fig. 5) obtained by the nanoindenter [8, 12, 13].

The reported Young’s modulus *E* from nanoindenter is calculated by

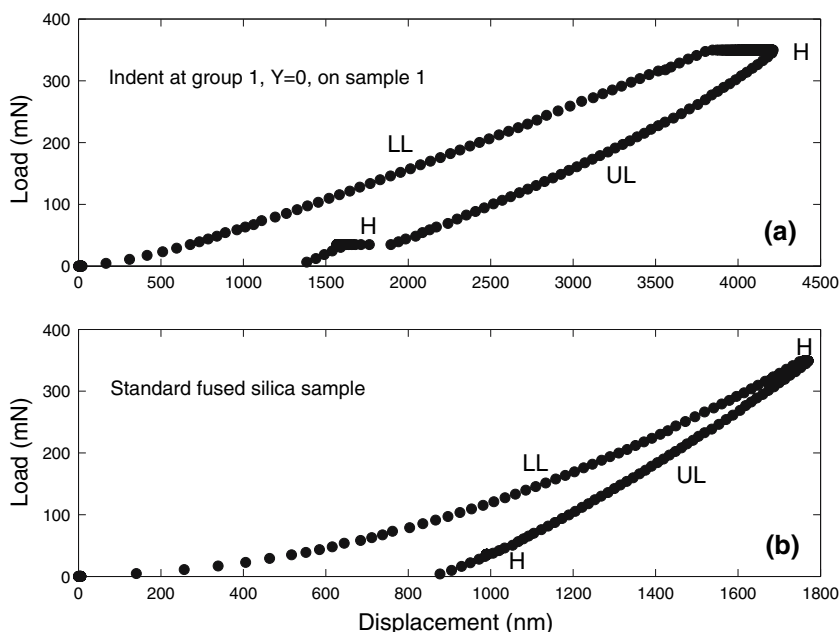
$$E = (1 - v_s^2) \left[ \frac{1}{E_c} - \frac{1 - v_i^2}{E_i} \right]^{-1}, \tag{1}$$

where *v<sub>s</sub>* = 0.16 and *v<sub>i</sub>* = 0.07 are the Poisson’s ratios for the fused silica sample and the diamond indenter, respectively, and *E<sub>i</sub>* = 1,141 GPa is the Young’s modulus of the indenter [12]. The measured composite modulus *E<sub>c</sub>* is defined as

$$E_c = \frac{\sqrt{\pi} S}{2 \sqrt{A_c}}, \tag{2}$$

where the contact area *A<sub>c</sub>* is a function of the contact depth *h<sub>c</sub>*, and *h<sub>c</sub>* = *h<sub>max</sub>*–0.75*P<sub>max</sub>*/*S*. *h<sub>max</sub>* and *P<sub>max</sub>* are

**Fig. 5** Load–displacement curves from nanoindentation. LL denotes Load Segment, H denotes Hold Segment, and UL denotes Unload Segment. (a) Indent at group 1,  $Y = 0$  on sample 1 after the first polishing. (b) An indent on the standard fused silica sample



the maximum displacement and the maximum load, respectively. The indent area function is given by

$$A_c = 24.56h_c^2 + \sum_{i=0}^7 C_i h_c^{2-i}, \tag{3}$$

where  $C_i$  are coefficients determined through a tip-area calibration [12] and in the present study  $C_0 = 0.0001518$ ,  $C_1 = 8.4204 \times 10^{-5}$ ,  $C_2 = 0.0016722$ ,  $C_3 =$

$0.00063492$ ,  $C_4 = 0.0031821$ ,  $C_5 = 0.00015795$ ,  $C_6 = 0.045883$ , and  $C_7 = 0.027571$ .

The contact stiffness  $S$  is the derivative of  $P$  with respect to  $h$  at  $h_{max}$  in the unloading part of the  $P-h$  curve. To calculate  $S$ , the upper 90% of the unloading curve is fitted by a least-squares fit to the following form:

$$P = a(h - h_f)^m, \tag{4}$$

**Fig. 6** Distributions of Young’s modulus on fused silica specimens after the second polishing (22 h). Improvement was seen but the average value of  $E$  was still 20% smaller than the literature value

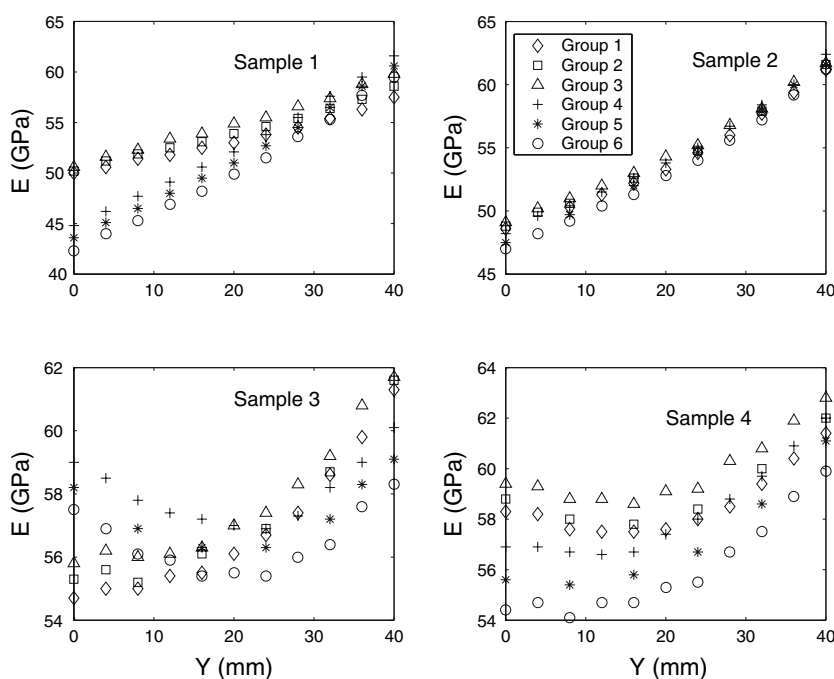
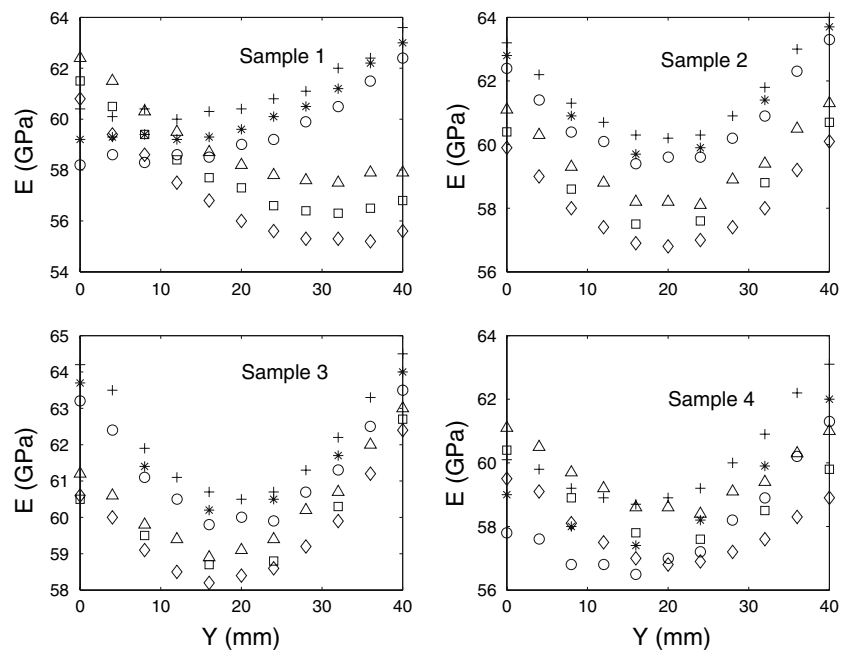


**Fig. 7** Distributions of Young’s modulus on fused silica specimens after the third polishing (1 week). The legend is the same as in Fig. 6



where  $a$ ,  $h_f$ , and  $m$  are the fitting parameters. Then  $S$  is obtained by

$$S = \left. \frac{dP}{dh} \right|_{h_{\max}} = am(h_{\max} - h_f)^{m-1}. \tag{5}$$

Similarly, the reported Berkovich hardness  $H$  from nanoindenter is defined by

$$H = \frac{P_{\max}}{A_c^2}. \tag{6}$$

Due to the arch bridge effect of the specimen, the displacement recorded in nanoindenter  $h$  actually includes two parts: the real displacement of indenter  $h_i$  and the deflection of the sample at the indenter  $h_s$ . If the sample is considered as a simple edge-supported beam, then  $h_s$  is given by

$$h_s = \frac{P(L - c)^2 c^2}{3LE_b I}, \tag{7}$$

where  $L$  is the length of the beam,  $I$  the moment of inertia,  $c$  the distance from indenter to one end of the beam, and  $E_b$  the Young’s modulus of bulk fused silica. In the present study,  $L = 77$  mm,  $I = 450$  mm<sup>4</sup>,  $E_b = 72.7$  GPa, and  $c = 18.5$  mm for indents at  $Y = 0$  mm.

In the correction process, the  $P$ – $h$  curve is corrected by subtracting  $h_s$ , then  $a$ ,  $h_f$ , and  $m$  in Eq. 4 are calculated from the unloading part of the corrected  $P$ – $h$  curve. After we get  $S$ ,  $h_c$ ,  $A_c$ , and  $E_c$  from the corrected  $P$ – $h$  curve, the corrected Young’s modulus and hardness are obtained by Eqs. 1 and 6, respectively.

**Table 2** Mean values and standard deviations of  $E$  and  $H$  of fused silica samples after each polishing

	First polishing		Second polishing		Third polishing	
	$E$ (GPa)	$H$ (GPa)	$E$ (GPa)	$H$ (GPa)	$E$ (GPa)	$H$ (GPa)
Sample 1	20.1 ± 11.1	3.48 ± 1.67	52.8 ± 4.5	8.10 ± 0.46	59.1 ± 2.0	8.78 ± 0.22
Sample 2	39.4 ± 13.0	6.07 ± 1.74	54.1 ± 4.3	8.41 ± 0.44	60.0 ± 1.8	8.97 ± 0.15
Sample 3	32.4 ± 9.6	5.56 ± 1.24	57.3 ± 1.7	8.68 ± 0.21	60.9 ± 1.6	9.09 ± 0.14
Sample 4	37.6 ± 10.3	6.25 ± 1.30	58.2 ± 2.2	8.74 ± 0.20	58.9 ± 1.5	8.83 ± 0.12
Standard sample	68.8 ± 0.2	9.54 ± 0.04				
Literature	71.5 <sup>a</sup> , 72.7 <sup>b</sup>	9.22 <sup>a</sup>				

Values from standard fused silica samples and literatures are also included for comparison

<sup>a</sup> Ref. [9]

<sup>b</sup> Ref. [10]

**Table 3** Mean values and standard deviations of corrected Young's modulus and Berkovich hardness of fused silica

	<i>E</i> (GPa)	<i>H</i> (GPa)
Sample 1	67.1 ± 2.6	9.09 ± 0.24
Sample 2	68.1 ± 1.7	9.28 ± 0.16
Sample 3	69.2 ± 1.4	9.41 ± 0.14
Sample 4	66.7 ± 1.4	9.14 ± 0.14

Table 3 shows the mean values and standard deviations of corrected Young's modulus and Berkovich hardness for each sample after the third polishing. The mean values and standard deviations of *E* and *H* from all the indents after the third polishing are  $59.7 \pm 1.9$  GPa and  $8.91 \pm 0.20$  GPa, respectively; while after correction, they become  $67.7 \pm 2.1$  GPa and  $9.22 \pm 0.21$  GPa. The corrected *E* and *H* are now in good agreement with those of the standard fused silica sample (see Table 2). This improvement is also a validation of the hypothesis of the arch bridge effect.

## Conclusions

After testing four fused silica samples that were polished three times by conventional pitch polishing, we found by using the nanoindentation technique that the surface Young's modulus and Berkovich hardness of these samples depended strongly on the quality of polishing. The longer the polishing time, the better the quality of the surface, the more uniform the distributions of *E* and *H*, and the closer to the literature values their mean values. However, even after polishing for 1 week, the measured Young's modulus was still 15% lower than the literature and standard fused silica sample values. This discrepancy originated from the flatness of the sample surfaces. Whenever polishing produces a flatness distribution of an arch bridge type,

the measured displacement of the indenter actually includes two parts: the real displacement of the indenter and the deflection of the sample under the load from the indenter. The elimination of the sample deflection effect results in a Young's modulus and Berkovich hardness in good agreement with those of a standard fused silica sample.

**Acknowledgments** This work was supported by the U.S. Department of Energy Office of Inertial Confinement Fusion under Cooperative Agreement No. DE-FC03-92SF19460, the University of Rochester, and the New York State Energy Research and Development Authority. The support of DOE does not constitute an endorsement by DOE of the views expressed in this article. One of the authors (L.Z.) gratefully acknowledges C. Pratt for help with nanoindentation tests and the Laboratory for Laser Energetics for a Horton Fellowship.

## References

1. Izumitani TS (1986) Optical glass. Amerian Institute of Physics, New York
2. Karow HH (1993) Fabricatin methods for precision optics. Wiley, New York
3. Lambropoulos JC, Xu S, Fang T (1997) Appl Optics 36:1501
4. Lambropoulos JC, Jacobs SD, Ruckman J (1999) Ceram Trans 102:113
5. Lambropoulos JC, Fang T, Funkenbusch P, Jacobs S, Cumbo M, Golini D (1996) Appl Optics 35:4448
6. Lambropoulos JC, Jacobs SD, Ruckman J (1998) In: Proceedings of 18th International Congress on glass. San Francisco, CA, United States, p 3057
7. Hirao K, Tomozawa M (1987) J Am Ceram Soc 70:497
8. Oliver WC, Pharr GM (2004) J Mater Res 19:3
9. Dahmani F, Lambropoulos JC, Schmid AW, Burns SJ, Pratt C (1998) J Mater Sci 33:4677
10. Product sheet for HPFS® 7980 standard grade, Corning, NY. <http://www.corning.com>, as on 14 November 2005
11. Duan K, Steinbrech RW (1998) J Eur Ceram Soc 18:87
12. Nano Indenter® Operating Instructions, Nano Instruments, Inc., Knoxville, TN (1996), version 2.2
13. Herrmann K, Jennett NM, Wegener W, Meneve J, Hasche K, Seemann R (2000) Thin Solid Films 377–378:394